journal

J. Am. Ceram. Soc., 88 [11] 3075–3080 (2005)
DOI: 10.1111/j.1551-2916.2005.00542.x

Oxidation of Polymer-Derived SiAlCN Ceramics

Yiguang Wang* and Linan An*,†

Advanced Materials Processing and Analysis Center, University of Central Florida, Orlando, Florida 32816

Yi Fan and Ligong Zhang

Laboratory of Excited State Process, Changchun Institute of Optics, Fine Mechanics and Physics, Chinese Academy of Sciences, Changchun 130032, China

Sarah Burton

Pacific Northwest National Laboratory, Richland, Washington 99352

Zhehong Gan

Center of Interdisciplinary Magnetic Resonance, National High Magnetic Field Laboratory, Tallahassee, Florida 32310

The oxidation behavior of polymer-derived amorphous SiAlCNs was studied in the temperature range of 900°–1200°C. The results revealed that while at 900°C the oxidation of the SiAlCNs follows typical parabolic kinetics, at higher temperatures the oxidation rates of the materials decrease with annealing time. Long-term oxidation rate of the SiAlCNs is much lower than the lowest values reported for chemical vapor deposition of SiC and Si_3N_4. Structures of the oxide scales were studied using solid-state nuclear magnetic resonance. We proposed that oxide scales formed for the SiAlCNs possess a unique network structure of the oxide scale in which aluminum atoms block the path of oxygen diffusion, thus lowering the oxidation rates. Such a unique structure was likely formed gradually with annealing time, leading to a continuous decrease in oxidation rate.

I. Introduction

Because of their excellent thermo-mechanical properties, Si-based ceramics are considered as one of the most promising candidates for high temperature structural applications. Recently, this class of materials has been alternatively synthesized by pyrolysis of polymeric precursors (referred to as polymer-derived ceramics (PDCs)). The materials in Si–C–N ternary or Si–C–N–M (M is the fourth element) quaternary systems have been prepared in the past decade.[1–3] The direct chemical-to-ceramic route of PDCs offers many advantages over traditional ceramic technologies based on powder processing. For example, the technique leads to a simple, cost-efficient and near-net shape approach to manufacture ceramic components and devices with inconvenient shapes, such as fibers, coatings, composites, micro-electro-mechanical systems, and nanostructures.[4–9] The technique also offers an opportunity to manipulate the structures and composites, and thereby the properties, of the final ceramics at atomic/nano-scale by tailoring the chemistry of the precursors. While synthesized at relatively low temperatures (pyrolysis is usually performed at 800°–1000°C), PDCs show excellent high temperature properties, such as resistance to creep[10–13] and large-scale crystallization.[2]

One of the key considerations for using silicon-based ceramics in high-temperature applications is that they can be oxidized to form an oxide layer, which results in material degradation. Oxidation behavior of PDCs was investigated in several previous studies.[14–23] It was found that the PDCs in Si–C–N and Si–B–C–N systems exhibited similar oxidation behavior as conventional silicon carbide and silicon nitride.[24] Recently, An *et al.*[25] reported that polymer-derived SiAlCN ceramics possess extremely high resistance to oxidation and hot-corrosion. At 1200°C, the oxidation rate measured for the PDC SiAlCN containing 1.4 at.% Al is an order of magnitude lower than the lowest rates measured from chemical vapor deposition (CVD) of SiC and Si_3N_4. The same material also shows great resistance to corrosion at 1200°C in either NaCl or water vapor environments.

In this paper, we report a detailed study on the oxidation behavior of the polymer-derived SiAlCN ceramics in the temperature range of 900°–1200°C. The oxidation kinetics are determined by measuring the thickness of the oxide layer as a function of annealing time. Structures of the oxide scales are studied using X-ray diffraction (XRD) and solid-state nuclear magnetic resonance (NMR). The effect of aluminum on the oxidation behavior of the SiAlCN ceramics is discussed.

II. Experimental Procedures

Fully dense SiAlCN discs were prepared using a novel pressure-assisted pyrolysis technique as described previously.[15,25] First, liquid-phased polyaluminasilazane precursors were synthesized by the reaction of commercially available polyurea (methylvinyl) silazanes (Ceraset, Kion, Huntingdon Valley, PA) and aluminum isopropoxide (AIs, Alfa Aesar, Ward Hill, MA) at 150°C for 4 h in flowing argon. The obtained liquid polyaluminasilazanes were mixed with 3 wt% dicumyl peroxide (Acros Organics, Morris Plains, NJ) as thermal initiator, and then cast into a Teflon tube of 0.5 in. inner diameter and solidified by heat-treatment at 150°C for 0.5 h. The obtained rods were cut into discs of 1 mm thick, and then cross-linked (400°C × 4 h) and pyrolyzed (1000°C × 4 h) in nitrogen. The cross-linking and pyrolysis were carried out under the isostatic pressure of 50 MPa to prevent the formation of cracks and pores within the samples. Two types of SiAlCNs containing different amounts of aluminum were synthesized by changing the ratio of Ceraset to AIs. For comparison, fully dense SiCN discs were

R. Naslain—contributing editor

Manuscript No. 20256. Received December 7, 2004; approved April 24, 2005.
Supported by Office of Research of UCF and "Hundred Person" program of the Chinese Academy of Science.
*Member, American Ceramic Society.
†Author to whom correspondence should be addressed. e-mail: lan@mail.ucf.edu

Table I. Precursors and Composition of Obtained Ceramics

Samples	Starting materials (CER:AIs weight ratio)	Ceramic compositions
SiAlCN-5	9.5:0.5	$SiAl_{0.02}C_{0.84}N_{0.90}$
SiAlCN-10	9:1	$SiAl_{0.04}C_{0.83}N_{0.93}$
SiCN	10:0	$SiC_{0.99}N_{0.85}$

AI, aluminum isopropoxide.

also prepared via the same procedure by using pure Ceraset as precursor. The chemical compositions of the SiCN and SiAlCN ceramics are listed in Table I.[26] The samples also contain ~3 wt% oxygen.

For oxidation studies, one side of the disk was polished to 0.5 μm finish using diamond-lapping films. The sample was then put in a quartz tube with the polished side faced up. The oxidation was carried out in a high-temperature tube furnace in flowing dry air at temperatures from 900° to 1200°C for various annealing times up to 200 h. Oxidation kinetics was determined by measuring the thickness of the oxide scale. First, the oxidized surface of the disk specimen was coated with the chromium protective layer and then cut into half. The cross-section of the specimen was polished to 0.5 μm finish. The polished cross-section was etched using Buffered Oxide Etchants (BOE, Ashland Chem., Boonton, NJ) to delineate the oxide layer from the substrate. The oxide scales were observed using scanning electron microscopy (SEM, JOEL 6400F, Tokyo, Japan) and their thickness was measured.

To study the structures of the oxide scales, powders of ~1–3 μm diameter were prepared for SiCN, SiAlCN-5, and SiAlCN-10. The powders were oxidized together with the disk samples. After oxidation, the powders were first analyzed using XRD. Further characterization of the oxidized powders was carried out by ^{29}Si solid-state magic angle spinning (MAS) NMR using a Chemagnetics 300 MHz Infinity spectrometer (Cambridge, UK) with a Larmor frequency of 59.6 MHz. A standard CP/MAS probe with a 7.5 mm pencil rotor was used. Sample spinning rates of 5 kHz were used for all the experiments. All spectra were acquired using a standard single pulse sequence with a tip angle of about 45° and a recycle delay time of 10 s with accumulation numbers varied from several hundred to 30 000 scans. The ^{29}Si chemical shifts were referenced to TTMS as external standard.

III. Results

The oxide scales were first examined using SEM and XRD (on powder samples). The results revealed that all oxide scales are amorphous, dense, and free of bubbles and cracks regardless of oxidation conditions and substrate materials. Figure 1(a) is a typical SEM micrograph showing the cross-section of an oxidized specimen. Figure 1(b) gives typical XRD patterns of oxidized powders, revealing the amorphous nature of the oxide scales.

Figure 2 plots the square of the thickness of the oxide scales as a function of annealing time for the SiCN and SiAlCNs at temperatures of (a) 900°, (b) 1000°, (c) 1100°, and (d) 1200°C, respectively. The slope of the curve in such a kind of plot is a parabolic rate constant according to the equation[27]

$$h^2 = k_p t \tag{1}$$

where h is the thickness of oxide scale, t the oxidation time, and k_p the parabolic rate constant. Several features can be seen from Fig. 2. At 900°C, all three materials follow typical parabolic oxidation kinetics—linear dependence of h^2 on annealing time. At this temperature the oxidation rate constants measured for three materials are comparable with each other (Table II). At higher temperatures (1000°–1200°C), the oxidation of the SiCN

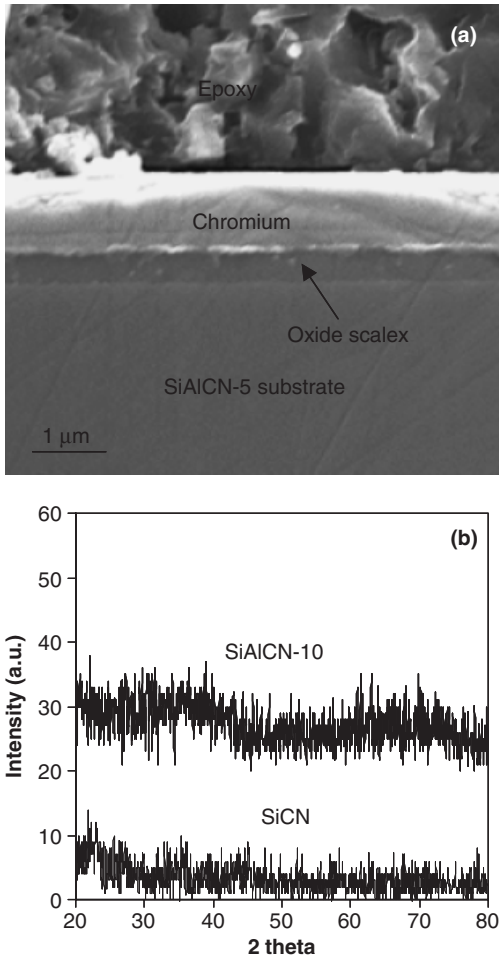

Fig. 1. (a) Scanning electron micrograph showing the morphology of the cross-section of the SiAlCN-5 oxidized at 1100°C for 20 h. (b) X-ray diffraction patterns of SiAlCN-10 (top) and SiCN (bottom) oxidized at 1200°C for 200 h.

still follows parabolic behavior. However, the two SiAlCNs show the decrease in the oxidation rates with annealing time. For the SiAlCNs, the oxidation data can be classified into three regions: the initial stage, the transition stage where oxidation rate decreases, and the steady stage where the oxidation rate becomes constant at a lower level. The oxidation rates of the initial stage (for 1000° and 1100°C, the first 50 h data were used; while for 1200°C, the first 20 h data were used) are close to that of the SiCN (Table II). For the samples oxidized at 1200°C, the steady-stage oxidation rates for the SiAlCN-5 and SiAlCN-10 were calculated using last 100 h data to be 0.3×10^{-18} and 0.025×10^{-18} m^2/s, respectively. These oxidation rates of the SiAlCN-5 and SiAlCN-10 are ~20 and 200 times lower than that of the SiCN (4.8×10^{-18} m^2/s), respectively.[25] The long-term oxidation rate of the SiAlCN-10 is even an order of magnitude lower than the lowest data measured from CVD SiC (0.55×10^{-18} m^2/s) and Si_3N_4 (0.22×10^{-18} m^2/s) obtained at similar conditions.[25] For the samples oxidized at 1000°C and 1100°C, it seems that the steady stage was not fully reached; the oxidation rate calculated by using the last 100 h data is higher than that obtained from samples oxidized at 1200°C.

The apparent activation energy of the oxidation can be calculated from the rate constants measured at the different temperatures using the Arrhenius equation:

$$k_p = A_0 \exp\left(-\frac{Q_A}{RT}\right) \tag{2}$$

where Q_A is the oxidation activation energy. Figure 3 plots the $\ln(k_p)$ as a function of reciprocal temperatures (the earlier-stage

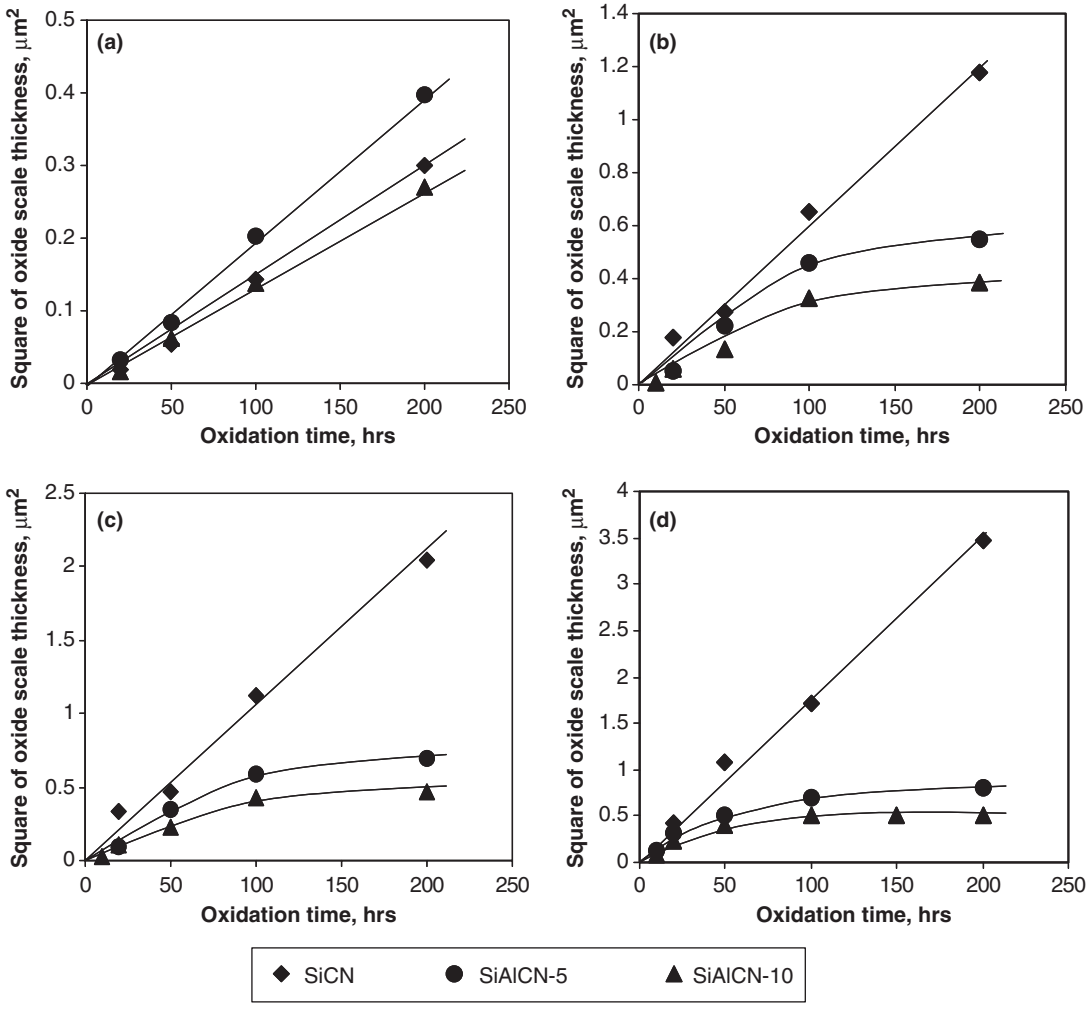

Fig. 2. Plots of the square of the oxide scale thickness as a function of annealing times for the SiCN, SiAlCN-5, and SiAlCN-10 at temperatures (a) 900°, (b) 1000°, (c) 1100°, and (d) 1200°C.

data listed in Table II are used for the SiAlCNs). It can be seen that fairly good linear relationships are obtained for all three materials. The activation energies calculated for the three materials are very close to each other (Table II), and are also similar to that for high purity SiC (such as CVD and/or single crystal SiC) and single crystal silicon, but much less than that of CVD silicon nitride.[28,29] This suggests that at low temperature or high temperature short-term, the oxidation of the SiAlCNs follows the same mechanism as the SiCN, which is similar to that for the oxidation of SiC.

Figure 4 shows ^{29}Si spectra of the SiCN and SiAlCN oxidized at different conditions. The signals between 0 and −75 ppm result from the un-oxidized substrates.[26] The spectra suggest that at 900°C, the oxide scale is thin and a significant amount of SiCN and SiAlCN substrates remain un-oxidized after 50 h annealing while at 1200°C, most of the substrates were oxidized. This result is consistent with oxide scale thickness measurement. The strong signal centered at −100 ppm is assigned to SiO_4 tetrahedral,[30] formed because of oxidation. It can be seen that the position of this signal remains unchanged for all samples, suggesting the aluminum atoms are not incorporated into the SiO_2 network.[31,32] Furthermore, the signals from the SiCN oxidized at all conditions and the SiAlCNs oxidized at 900°C show

Table II. The Parabolic Rate Constants and Activation Energies for the SiCN and SiAlCNs

	Parabolic rate constants ($\times 10^{18}$ m^2/s)				
Materials	900°C	1000°C	1100°C	1200°C	Activation energy (kJ/mol)
SiCN	0.39	1.3	2.8	4.8	120
SiAlCN-5	0.56	1.2	2.3	5.3	115
SiAlCN-10	0.39	0.98	1.6	3.9	115

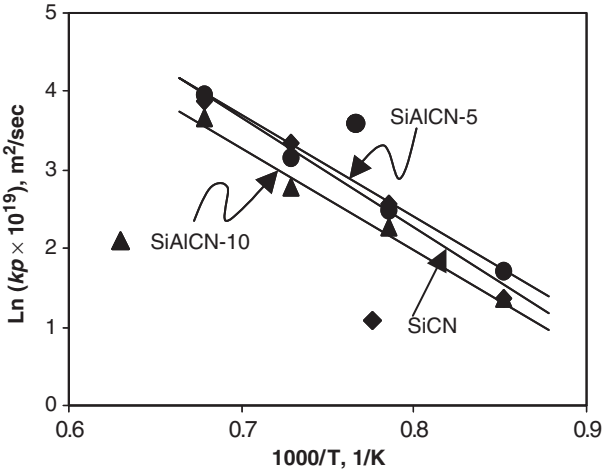

Fig. 3. Plot of log parabolic rate constants as a function of reciprocal of temperatures for the SiCN, SiAlCN-5, and SiAlCN-10. The rate constants of the SiAlCN-5 and SiAlCN-10 for temperatures higher than 1000°C were calculated using initial stage data.

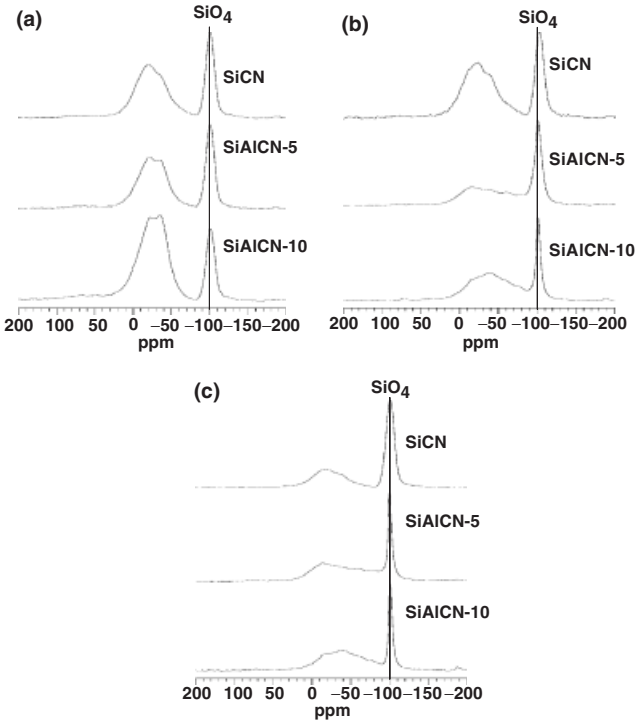

Fig. 4. ^{29}Si NMR spectra of the SiCN and SiAlCNs oxidized at (a) 900°C × 50 h, (b) 1200°C × 20 h, and (c) 1200°C × 200 h.

similar shape, suggesting the SiO_2 network structures formed under these conditions are similar to each other. However, at 1200°C the signals from SiAlCN specimens are sharpened with annealing time, suggesting that the SO_2 structures become more ordered. The results also suggest that the structures of the SiO_2 scale formed on the SiAlCNs are rearranged with time at higher oxidation temperatures.

IV. Discussion

As described above, polymer-derived SiAlCN ceramics exhibited unique oxidation behaviors, including: (i) the oxidation rate decreases with annealing time, (ii) the steady-stage oxidation rate measured for SiAlCN-10 at 1200°C is ~10 times lower than the lowest values reported for CVD SiC and Si_3N_4 obtained at similar conditions, and (iii) the oxidation rate decreases with increasing aluminum content. Here, we would like to emphasize that the decrease in oxidation rates with time observed for the SiAlCNs is not the same as that observed in porous materials through weight change measurement.[18,33] In porous materials, the decrease in weight gain is because of pore sealing and can only be detected by measuring weight change.[15] In contrast, the oxidation rates shown in Fig. 2 were obtained by directly measuring the thickness of oxide scale.

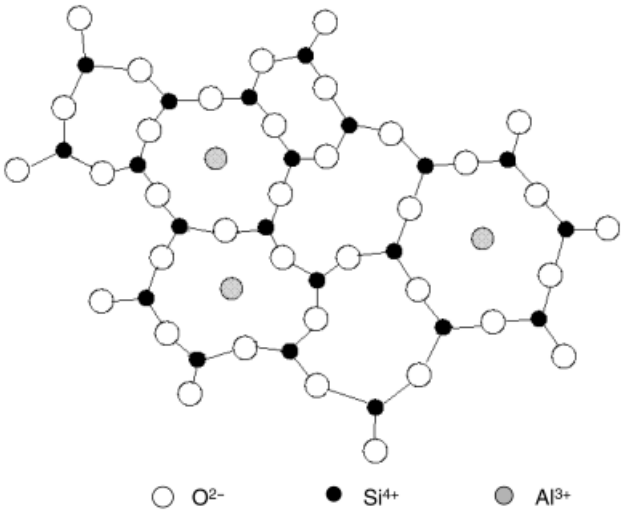

Fig. 5. Two-dimensional schematic showing the proposed structure of silica oxide scale, in which aluminum atoms sit in the center of the 6-membered rings of Si–O to block the diffusion of oxygen.

The oxidation rate of silicon-based materials is controlled by oxygen diffusion through the oxide layer (under the current condition—temperatures $\leq$1200°C, oxygen diffusion occurs by interstitial transportation of oxygen molecules),[28,29] leading to parabolic kinetics. For silicon and silicon carbide, the oxide scale comprises of a single layer of SiO_2 while for silicon nitride, a bi-layer structure consisting of SiO_2 outer-layer and Si_2N_2O middle-layer between the SiO_2 layer and the substrate was observed.[34] As the oxynitride layer has a lower permeability to oxygen than SiO_2 and thus acts as a diffusion barrier,[34,35] silicon nitride has a lower oxidation rate and higher activation energy. However, the theory of the silicon oxynitride layer is not applicable to the SiAlCNs as (i) the oxynitride layer was not observed in the oxide scales, (ii) the oxidation rate of the SiAlCN is even much lower than that for Si_3N_4, and (iii) the undoped SiCN exhibits oxidation behavior similar to that of SiC.

Consequently, the only possible explanation for the decrease in the oxidation rate of the SiAlCNs is that the aluminum atoms modified the network structure of the oxide scale. Here let us first summarize the current understanding of silica network structure and oxygen diffusion within it. The structure of amorphous silica can be characterized by connected rings comprising of SiO_4 tetrahedral,[36] which gives a medium-range ordering to the material. Raman spectrum studies[37–39] indicated that the majority of these rings are 6-membered or higher; only a few percentages of them are 3- or 4-membered. Previous study[40] revealed that the calculated activation energy of oxygen molecules passing through 6-membered rings was comparable with that measured for the oxidation of silicon/silicon carbide. These results suggest that the 6-membered rings are the barriers for the diffusion of oxygen molecules in amorphous silica. Among all simple oxides, SiO_2 possesses lowest oxygen permeability.[41] The presence of impurities usually damages the network structure of the SiO_2 and results in the increase in oxygen diffusion and higher oxidation rates[28,29] by providing an easier diffusion path.

The XRD study indicates that all oxide scales in this study are amorphous. The ^{29}Si NMR results (Fig. 4) suggest that the oxide scale formed on the surface of the SiAlCN samples became more ordered with annealing time (the signal corresponding to SiO_4 sharpened with time). Here we argue that the ordering of the oxide scale cannot cause the decrease in oxygen diffusion. The ordering can decrease the diffusion by decreasing the average free volume only when the diffusion is controlled by free volume mechanism. In case of oxygen molecules' diffusion through interstitials of silica glass, the barrier is the 6-membered SiO_4 rings.[40] The size of these rings should not be changed (at least not significantly) with ordering, thus oxygen transportation should not be affected. We can even extend this argument to crystalline silica, in which interstitial oxygen molecule diffusion should not be much different from that in amorphous form as in both cases it is the 6-membered rings that controlled the diffusion. Recently, Ramberg and Worrell[42] experimentally demonstrated that there is no difference between the rates of interstitial oxygen transport in amorphous SiO_2 and in β-cristobalite.

In this paper, we propose that the oxide scale formed on the SiAlCNs has a unique network structure, namely aluminum atoms (at least part of them) sit in the center of the 6-membered rings (Fig. 5). These aluminum atoms block the path of oxygen diffusion so that oxygen molecules have to take a longer transportation path, leading to lower oxidation rate for SiAlCNs. While the aluminum content is relatively low (ratio of Al to Si is 0.02 and 0.04 for SiAlCN-5 and SiAlCN-10, respectively), the

number of the blocked rings may already reach percolation values. We further propose that the unique network structure of Al-blocking 6-membered Si–O rings is formed gradually with time through structural rearrangement, as evidenced in the NMR spectra (Fig. 4). The rearrangement requires high temperature and time for the kinetic reason. At 900°C or initial stage of higher-temperatures, the rearrangement did not occur or just started because of the low temperature or shorter time, thus the oxidation of the SiAlCNs is similar to that for the SiCN. At higher temperatures, the structural rearrangement leads to the decrease in oxidation rate. This model can also easily explain the fact that the oxidation rates decrease with increasing aluminum content because more rings are blocked.

Here we like to compare the proposed model with other Al-containing Si-based ceramics. The decrease in oxidation rate with time has also been observed previously in sialon ceramics at a temperature range of 1400°–1600°C.[43,44] The authors attributed this to the formation of a fused silica layer containing octahedral Al.[43] However, the reason that octahedral Al can slow the oxidation was not discussed. It is possible that these aluminum atoms also sit in the center of 6-membered SiO_4 rings. Oxidation behavior of PDCs SiBCNAl ceramics has been reported recently.[45,46] These studies revealed that compared with aluminum-free SiBCNs, aluminum-containing SiBCNAl exhibited a slight higher oxidation rate. But aluminum did help to improve the oxide scale quality in terms of adhesion, cracking, bubble formation, and crystallization. Compared with our materials, these previously studied materials contain boron and higher Al-to-Si ratios. This could be reason why improved oxidation resistance was not observed in these SiBCNAl materials.

Finally, we would like to make following comments:

(i) The formation of the unusual diffusion-blacking structure should not be limited to the polymer-derived SiAlCN system. Any aluminum-containing silicon-based system may have the chance to form such structure if the aluminum distribution is uniform initially.

(ii) The formation of the blocking structure should not be limited to aluminum-doping only. Other elements could also sit in the center of the ring or cage to block oxygen diffusion and reduce oxidation rate.

(iii) There should be a limitation on aluminum content to form effective blocking structures because the amount of atoms that can be accepted by the suitable sites may be limited, similar to solubility in solid solution. Extra atoms may cause the structural relaxation to cancel the blocking effect or even increase oxygen diffusion by providing an alternative diffusion path.

V. Summary

The oxidation behaviors of polymer-derived SiAlCN ceramics were studied in the temperature range of 900°–1200°C. The oxidation kinetic measurement revealed that at 900°C, the oxidation of the SiAlCNs is similar to the SiCN, following parabolic kinetics. At higher temperatures, the oxidation rates of the SiAlCNs decrease with annealing time. NMR study revealed that the network structure of the vitreous silica formed during oxidation is changed with annealing time.

A unique structural model in which aluminum atoms sit in the middle of the 6-memebered Si–O rings is proposed to account for the observed oxidation behavior of the SiAlCN. The further research is undergoing to examine this model by measuring other properties of the oxide scales.

References

[1]R. Riedel, G. Passing, H. Schonfelder, and R. J. Brook, "Synthesis of Dense Silicon-Based Ceramics at Low-Temperatures," *Nature*, **35**, 714–6 (1992).

[2]R. Riedel, A. Kienzle, W. Dressler, L. Ruwisch, J. Bill, and F. Aldinger, "A Silicoboron Carbonotride Ceramics Stable to 2000 Degrees C," *Nature*, **382**, 796–8 (1996).

[3]E. Kroke, Y. L. Li, C. Konetschny, E. Lecomte, C. Fasel, and R. Riedel, "Silazane Derived Ceramics and Related Materials," *Mater. Sci. Eng. R*, **26**, 97–199 (2000).

[4]S. Yajima, Y. Hasegawa, K. Okamura, and T. Matsuzawa, "Development of High-Tensile-Strength Silicon Carbide Fiber Using an Organosilicon Polymer Precursor," *Nature*, **273**, 525–7 (1978).

[5]L. An, W. Xu, S. Rajagopalan, C. Wang, H. Wang, J. Kapat, L. Chow, Y. Fan, L. Zhang, D. Jiang, B. Guo, J. Liang, and R. Vaidyanathan, "Carbon Nanotube Reinforced Polymer-Derived Ceramic Composites," *Adv. Mater.*, **16** [22] 2036–40 (2004).

[6]P. Greil, "Polymer-Derived Engineering Ceramics," *Adv. Eng. Mater.*, **2** [6] 339–48 (2000).

[7]L. Liew, W. Zhang, L. An, S. Shah, R. Lou, Y. Liu, T. Cross, K. Anseth, V. Bright, and R. Raj, "Ceramic MEMS—New Materials, Innovative Processing and Futuristic Applications," *Am. Ceram. Soc. Bull.*, **80** [5] 25–30 (2001).

[8]W. Yang, H. Miao, Z. Xie, L. Zhang, and L. An, "Synthesis of Silicon Carbide Nanorods by Catalyst-Assisted Pyrolysis of Polymeric Precursor," *Chem. Phys. Lett.*, **383** [5–6] 441–4 (2004).

[9]W. Yang, Z. Xie, H. Miao, L. Zhang, H. Ji, and L. An, "Synthesis of Single-Crystalline Silicon Nitride Nanobelts via Catalyst-Assisted Pyrolysis of a Polysilazane," *J. Am. Ceram. Soc.*, **88** [2] 466–469 (2005).

[10]L. An, R. Riedel, C. Konetschny, H. -J. Kleebe, and R. Raj, "Newtonian Viscosity of Amorphous Silicon Carbonitride at High Temperature," *J. Am. Ceram. Soc.*, **81**, 1349–52 (1998).

[11]R. Riedel, L. M. Ruwisch, L. An, and R. Raj, "Amorphous Silicoboron Carbonitride Ceramics with Anomalously High Resistance to Creep," *J. Am. Ceram. Soc.*, **81**, 3341–4 (1998).

[12]G. Thum, J. Canel, J. Bill, and F. Aldinger, "Compression Creep Behavior of Precursor-Derived Si–C–N Ceramics," *J. Eur. Ceram. Soc.*, **19**, 2317–23 (1999).

[13]M. Christ, G. Thurn, M. Weinmann, J. Bill, and F. Aldinger, "High Temperature Mechanical Properties of Si–B–C–N-Precursor-Derived Amorphous Ceramics and the Applicability of Deformation Models Developed for Metallic Glasses," *J. Am. Ceram. Soc.*, **83** [12] 3025–32 (2000).

[14]A. Saha, S. Shah, and R. Raj, "Oxidation Behavior of SiCN–ZrO_2 Fiber Prepared from Aloxide-Modified Silazane," *J. Am. Ceram. Soc.*, **87** [8] 1556–8 (2004).

[15]L. Bharadwaj, Y. Fan, L. Zhang, D. Jiang, and L. An, "Oxidation Behavior of a Fully Dense Polymer-Derived Amorphous Silicon Carbonitride Ceramic," *J. Am. Ceram. Soc.*, **87** [3] 483–6 (2004).

[16]E. Butchereit, K. G. Nickel, and A. Muller, "Precursor-Derived Si–B–C–N Ceramics: Oxidation Kinetics," *J. Am. Cerm. Soc.*, **84**, 2184–8 (2001).

[17]E. Butchereit and K. G. Nickel, "Comparison of the Oxidation Kinetics of Boron Free and Boron Containing Precursor Derived Ceramics"; pp. 112–3 in *High Temperature Corrosion and Materials Chemistry III*, Edited by E. J. Opila, *et al.* The Electrochemical Society, Washington, DC, 2001.

[18]R. Raj, L. An, S. Shah, R. Riedel, C. Fasel, and H. J. Kleebe, "Oxidation Kinetics of an Amorphous Silicon Carbonitride Ceramic," *J. Am. Ceram. Soc.*, **84**, 1803–10 (2001).

[19]K. G. Nickel, "Corrosion: No Problem for Precursor-Derived Covalent Ceramics"; pp. 188–96 in *Precursor-Derived Ceramics: Synthesis, Structure and High Temperature Mechanical Properties*, Edited by J. Bill, F. Wakai, and F. Aldinger. Wiley VCH, New York, NY, 1999.

[20]H. P. Baldus and M. Jansen, "Novel High-Performance Ceramics–Amorphous Inorganic Networks from Molecular Precursors," *Angew. Chem. Int. Ed. Engl.*, **36**, 328–43 (1997).

[21]H. P. Baldus, G. Passing, D. Sporn, and A. Thierauf, "Si–B–(N,C) a New Ceramic Material for High Performance Applications"; pp. 75–84 in *High-Temperature Ceramic Matrix Composites II: Manufacturing and Materials Development. Ceramic Transactions*, Vol. 56, Edited by A. G. Evans and R. Naslain. American Ceramic Society, Westerville, OH, 1995.

[22]G. Mocaer, D. Chollon, R. Pailler, L. Filipuzzi, and R. Naslain, "Si–C–N Ceramics with a High Microstructural Stability Elaborated from the Pyrolysis of New Polycarbosilazane Precursors, Part V: Oxidation Kinetics of Model Filaments," *J. Mater. Sci.*, **28**, 3059–68 (1993).

[23]D. Bahloul, M. Pereira, and P. Goursat, "Silicon Carbonitride Derived from an Organometallic Precursor: Influence of the Microstructure on the Oxidation Behavior," *Ceram. Int.*, **18**, 1–9 (1992).

[24]N. S. Jacobson, E. J. Opila, and K. N. Lee, "Oxidation and Corrosion of Ceramics and Ceramic Matrix Composites," *Curr. Opin. Solid State Mater. Sci.*, **5**, 301–9 (2001).

[25]L. An, Y. Wang, L. Bharadwaj, W. Xu, Y. Fan, L. Zhang, D. Jiang, Y. Sohn, V. Desai, J. Kapat, and L. Chow, "Amorphous Silicoaluminum Carbonitride with Ultrahigh Oxidation/Hot-Corrosion Resistance," *Adv. Eng. Mater.*, **6** [5] 337–40 (2004).

[26]A. Dhamne, W. Xu, B. Fookes, Y. Fan, L. Zhang, S. Burton, J. Hu, J. Ford, and L. An, "Polymer–Ceramic Conversion of Polyaluminasilazanes for Amorphous SiAlCN Ceramic," *J. Am. Ceram. Soc.* (accepted).

[27]B. E. Deal and A. S. Grove, "General Relationship for Thermal Oxidation of Silicon," *J. Appl. Phys.*, **36**, 3770 (1965).

[28]N. S. Jacobson, "Corrosion of Silicon-Based Ceramics in Combustion Environments," *J. Am. Ceram. Soc.*, **76**, 3–28 (1993).

[29]R. E. Tressler, "Theory and Experiment in Corrosion of Advanced Ceramics"; pp. 3–22 in *Corrosion of Advanced Ceramics*, Edited by K. G. Nickel. Kluwer Academic, Boston, MA 1994.

[30]K. J. D. Mackenzie and M. E. Smith, "^{29}Si NMR"; pp. 205–14 in *Multinuclear Solid-State NMR of Inorganic Materials*. Pergamon, New York 2002.

[31]M. Schmucker, K. J. D. MacKenzie, H. Schneider, and R. Meinhold, "NMR Studies on Rapidly Solidified SiO_2–Al_2O_3 and SiO_2–Al_2O_3–Na_2O–Glasses," *J. Non-Cryst. Solids*, **217** [1] 99–105 (1997).

[32]Z. H. Luan, C. F. Cheng, W. Z. Zhou, and J. Klinowski, "Mesopore Molecular Sieve MCM-41 Containing Framework Aluminum," *J. Phys. Chem.*, **99** [3] 1018–24 (1995).

[33]F. Porz and F. Thummler, "Oxidation Mechanisms of Porous Silicon Nitride," *J. Mater. Sci.*, **19**, 1283–95 (1984).

[34]L. U. J. T. Ogbuji, "Role of Si_2N_2O in the Passive Oxidation of Chemically-Vapor-Deposited Si_3N_4," *J. Am. Ceram. Soc.*, **75** [11] 2995–3000 (1992).
[35]H. Du, R. E. Tressler, and K. E. Spear, "Thermodynamics of the Si–N–O System and Kinetic Modeling of Oxidation of Si_3N_4," *J. Electrochem. Soc.*, **136** [11] 3210–5 (1989).
[36]S. V. King, "Ring Configurations in a Random Network Model of Vitreous Silica," *Nature*, **213**, 1112–3 (1967).
[37]P. Umari and A. Pasquarello, "Modeling of the Raman Spectrum of Vitreous Silica: Concentration of Small Ring Structures," *Physica B.*, **316–317**, 572–4 (2002).
[38]J. P. Rino, I. Ebbsjö, R. K. Kalia, A. Nakano, and P. Vashishta, "Structure of Rings in Vitreous SiO_2," *Phys. Rev. B*, **47** [6] 3053–62 (1993).
[39]K. Vollmayr, W. Kob, and K. Binder, "Cooling-Rate Effects in Amorphous Silica: A Computer-Simulation Study," *Phys. Rev. B.*, **54** [22] 15808–27 (1996).
[40]T. Bakos, S. N. Rashkeev, and S. T. Pantelides, "Reactions and Diffusion of Water and Oxygen Molecules in Amorphous SiO_2," *Phys. Rev. Lett.*, **88**, 055508 (2002).
[41]M. P. Brady, B. A. Pint, P. F. Tortorelli, I. G. Wright, and R. J. Hanrahan Jr., "High-Temperature Oxidation and Corrosion of Intermetallics," *Mater. Sci. Technol.*, Vol. II, 229–325 (2000).
[42]C. E. Ramberg and W. L. Worrell, "Oxygen Transport in Silica at High Temperatures: Implication of Oxidation Kinetics," *J. Am. Ceram. Soc.*, **84** [11] 2607–16 (2001).
[43]K. J. D. MacKenzie, C. M. Sheppard, G. C. Barris, A. M. Mills, S. Shimada, and H. Kiyono, "Kinetics and Mechanism of Thermal Oxidation of Sialon Powders," *Thermochim. Acta*, **318**, 91–100 (1998).
[44]T. Ekström and M. Nygren, "SiAlON Ceramics," *J. Am. Ceram. Soc.*, **75** [2] 259–76 (1992).
[45]A Müller, P. Gerstel, E. Butchereit, K. G. Nickel, and F. Aldinger, "Si/B/C/N/Al Precursor-Derived Ceramics: Synthesis, High Temperature Behavior and Oxidation Resistance," *J. Eur. Ceram. Soc.*, **24**, 3409–17 (2004).
[46]E. Butchereit and K. G. Nickel, "Beneficial Effect of Aluminum on the Oxidation Behavior of Precursor-Derived Ceramics"; pp. 325–38 in *High Temperature Corrosion and Materials Chemistry IV*, Edited by E. Opila, *et al.* The Electrochemical Society, Washington, DC, 2003. □